

Field-Effect Transistor based on Surface Negative Refraction in Weyl Nanowires

Guangze Chen, Wei Chen,* and Oded Zilberberg
Institute for Theoretical Physics, ETH Zurich, 8093 Zurich, Switzerland
 (Dated: August 30, 2019)

Weyl semimetals are characterized by their bulk Weyl points – conical band touching points that carry a topological monopole charge – and Fermi arc states that span between the Weyl points on the surface of the material. Recently, significant progress has been made towards understanding and measuring the physical properties of Weyl semimetals. Yet, potential applications remain relatively sparse. Here, we propose Weyl semimetal nanowires as field-effect transistors, dubbed WEYLFETs. Specifically, applying gradient gate voltage along the nanowire, an electrical field is generated that effectively tilts the open surfaces, thus, varying the relative orientation between Fermi arcs on different surfaces. As a result, perfect negative refraction between adjacent surfaces can occur and longitudinal conductance along the wire is suppressed. The WEYLFET offers a high on/off ratio with low power consumption. Adverse effects due to dispersive Fermi arcs and surface disorder are studied.

Field-effect transistors (FETs) are electronic devices that use an electric field to control the flow of current through the device [1]. There is a wide variety of materials and platforms used for various use cases of FETs; the majority thereof rely on semiconductor devices where the conduction channel can be switched off using an external gate. The conduction channel lies in the bulk of the semiconductor and early challenges in FET production concerned with surface passivation in order to overcome surface effects that prevented the gating from reaching the bulk [1]. In parallel, low-power FETs' applications are in constant development where new materials and reduced dimensionality of the conduction channel play a crucial role [2, 3]. Most recently, the progress of topological materials has opened a new avenue towards this goal based on the dissipationless chiral edge channels of the quantum anomalous Hall effect [4–11].

Weyl semimetals are a class of 3D materials with conduction and valence bands that linearly touch at isolated points of the bulk spectrum [12–17]. The touching points are so-called Weyl points, around which the electronic states can be effectively described by the Weyl equation [12]. Each Weyl point carries a monopole charge of Berry curvature, thus splitting momentum space into different regions of gapped spectra with different topology [12, 18]. These unique bulk properties lead to electron chirality that offers potential applications as a bulk photovoltaic effect [19, 20].

In parallel, the nontrivial bulk topology has a corresponding boundary effect in the form of Fermi arcs that appear in the surface Brillouin zone [12], which were recently observed experimentally [21–32]. These arcs have an open cut at the chemical potential, leading to directional transport on the surface. Furthermore, depending on the orientation of the surface, the Fermi arcs are projected from the bulk Weyl points differently [33]. This can lead to tunable surface configurations where negative refraction may occur between different surfaces of the material [34].

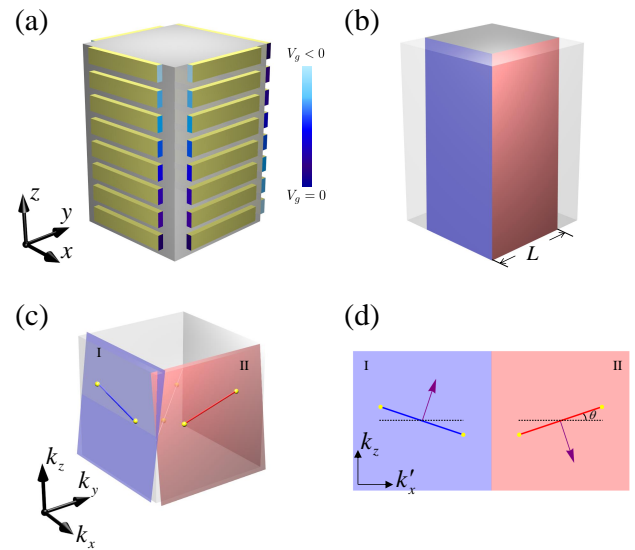


FIG. 1. Schematic of the Weyl semimetal field-effect transistor (WEYLFET). (a) The device is made of a Weyl semimetal nanowire (bulk core). Isolated metal gates are fabricated on top of the wire's surfaces with opposite gate-voltage gradients on the front and back surfaces (mind the colorbar). (b) The gate voltage effectively results in tilting of the open surfaces. (c) The tilted surface Brillouin zones lead to tilting of the Fermi arcs. (d) Two adjacent surfaces with opposite rotation of Fermi arcs induce negative refraction.

In this letter, we propose a new type of FET based on field-controlled surface negative refraction in a Weyl nanowire, or in short a WEYLFET. We consider a Weyl semimetal nanowire covered by isolated metal gates on top of each surface, see Fig. 1(a). By imposing a slanted electric potential along the nanowire, the redistribution of the electrons in the nanowire adjusts the bearings of the open surfaces, see Fig. 1(b). For nanowires with properly chosen surface bearings relative to the orientation of the bulk Weyl nodes, the electric potential results

in an effective tilting of the Fermi arc in each surface Brillouin zone, see Fig. 1(c). Such relative tilting of Fermi arcs in the surface Brillouin zone can lead to perfect negative refraction between adjacent surfaces [33, 34], see Fig. 1(d). The surface negative refraction considerably suppresses the conduction of electrons along the nanowire, i.e., for linear Fermi arcs, this effect produces a sharp electrically-tunable on/off switch of the conductance. We analyze the adverse impact of dispersive Fermi arcs, and the influence of surface disorder. Our proposal offers (i) a robust surface effect that does not necessitate passivation, (ii) reduced dissipation due to the backscattering-free channels, and (iii) a tunable sharp on/off switch, all of which make our proposed device a promising candidate for a low-power (WEYL-)FET.

In order to realize a WEYL FET with high on/off ratio, it is essential to have ideal Weyl semimetals [35, 36], in which the Fermi energy crosses both Weyl points and the transport is dominated by surface electrons. Furthermore, we consider sufficiently small tilting angles, such that reduction of the cross-section area of the nanowire is negligible. Hence, the main effect of the slanted gate voltage is the tilting of the orientation of the Fermi arcs, and the WEYL FET is controlled by the modulated surface transport.

Instead of studying nanowires with various surface bearings, we focus on the bulk Weyl nanowire with a general orientation of Weyl points, while retaining the same termination configuration of the nanowire. This approach is beneficial for the numerical study of the surface states [33]. More concretely, we consider the minimal inversion (\mathcal{P})-symmetric Weyl semimetal with two generally orientated Weyl points [37]. We start with a Weyl semimetal with two Weyl points at $\pm(0, 0, k_0)$:

$$H(\mathbf{k}) = \hbar v(k_x \sigma_x + k_y \sigma_y) + M(k_0^2 - \mathbf{k}^2)\sigma_z, \quad (1)$$

where v , M and k_0 are parameters, $\mathbf{k} = (k_x, k_y, k_z)$ is the wave vector, and $\sigma_{x,y,z}$ are Pauli matrices acting on the pseudospin space. The general orientation of Weyl points is achieved using the rotational transformation U to the effective Hamiltonian $\mathcal{H}(\mathbf{k}) = H(U^{-1}\mathbf{k})$, e.g., the rotation by an angle φ around the axis $k_x = k_y, k_z = 0$ yields two Weyl points located at $\pm k_0(-\frac{\sin \varphi}{\sqrt{2}}, \frac{\sin \varphi}{\sqrt{2}}, \cos \varphi)$. We consider a nanowire along the z -direction with a square cross section with side length L , cf. Fig. 1(b). We take $\varphi_0 = \pi/2$ as the starting point in the absence of applied gate voltage V . The gating results in rotation of the Weyl points with angle $\varphi_0 - \varphi(V)$. It corresponds to a tilting of the Fermi arcs by an angle $\theta(V) = \varphi_0 - \tan^{-1}[\tan \varphi(V)/\sqrt{2}]$ in the surface Brillouin zone [33] [Fig. 1(d)].

For convenience, we unfold the four open surfaces into the $x-z$ plane and label the longitudinal (transverse) momentum by k_z (k'_x), see Fig. 1(d). The Fermi arcs on surfaces I and II can be described by the effective

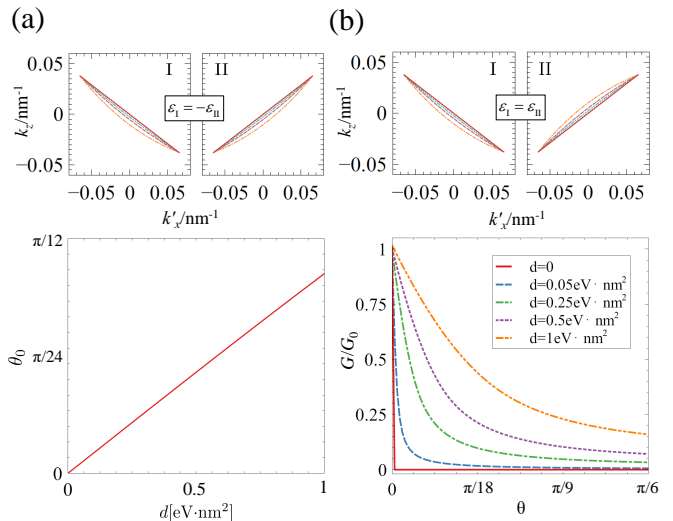


FIG. 2. (a) The Fermi arcs defined by Eq. (2) with different dispersion strength d [labelled by the legend in (b)] (upper panel) and the switch-off angle θ_0 as a function of d (lower panel), with $\varepsilon_I = -\varepsilon_{II}$. (b) The Fermi arcs defined by Eq. (2) (upper panel) and the conductance G [Eq. (3)] as a function of θ (lower panel) with different dispersion d , and $\varepsilon_I = \varepsilon_{II}$. All results are obtained with parameters: $v_0 = 10^6$ m/s and $k_0 = 0.1$ nm $^{-1}$.

Hamiltonian

$$H_{I,II}(\mathbf{k}) = \hbar v_0(\sin \theta k'_x \pm \cos \theta k_z) + \varepsilon_{I,II}(\mathbf{k}), \quad (2)$$

where $\mathbf{k} = (k'_x, k_z)$ is the in-plane momentum, v_0 is the velocity of the surface states, and “ \pm ” corresponds to surfaces I and II, respectively. $\varepsilon_{I,II}$ is the dispersion term, which introduces finite curvature to the Fermi arcs as in real materials. When $\varepsilon_{I,II} = 0$, the straight Fermi arcs defined by $H_{I,II} = \sin \theta k'_x \pm \cos \theta k_z \equiv 0$ have end points at $\pm k_0 [-(\sin \varphi)/\sqrt{2}, \cos \varphi]$ for surface I, and at $\pm k_0 [(\sin \varphi)/\sqrt{2}, \cos \varphi]$ for surface II [33]. The two Fermi arcs have opposite tilting, see Figs. 1(c) and (d). For a finite tilting angle ($\theta < \pi/2$), the velocity in the z -direction is inverted as the electrons transfer through the boundary between surfaces I and II, leading to negative refraction, see Fig. 1(d). This results in full suppression of electrons’ flow along the z -direction. This is the key mechanism behind the WEYL FET, i.e., even infinitesimal gating should lead to an on/off control of the electronic transport.

More realistically, Weyl semimetals exhibit dispersive Fermi arcs that depend on both bulk and surface details. Here, we consider a parabolic dispersion $|\varepsilon_{I,II}| = d[k_0^2(1 - \frac{1}{2} \sin^2 \varphi) - k_x'^2 - k_z^2]$, where the overall sign of the dispersive correction on each surface can change. By tuning the dispersion strength $|d|$, the Fermi arcs become curved [cf. Figs. 2(a) and (b)], as observed in real materials. Correspondingly, the electronic group velocities $\mathbf{v}^{I,II}(\mathbf{k}) = (v_x^{I,II}, v_z^{I,II})$ for the two surface states become

\mathbf{k} -dependent. The zero-energy single-spin conductance along the wire can be evaluated quasi-classically by

$$G = 2Le^2\rho_0\bar{v}_z, \quad \bar{v}_z = \int_{-k_x^0}^{k_x^0} \frac{dk'_x}{2k_x^0} v_z(k'_x), \quad (3)$$

with

$$v_z(k'_x) = \frac{v_z^I(k'_x, k_z)v_x^{\text{II}}(k'_{x2}, k_z) + v_z^{\text{II}}(k'_{x2}, k_z)v_x^I(k'_x, k_z)}{v_x^I(k'_x, k_z) + v_x^{\text{II}}(k'_{x2}, k_z)}, \quad (4)$$

where the integral is taken over the incident states of surface I and the velocity $v^{\text{II}}(k'_{x2}, k_z)$ is determined by the conservation of k_z during the negative refraction. In the above expressions, ρ_0 is the surface density of states per unit area, \bar{v}_z is the average velocity in the z -direction, and $\pm k_x^0$ are the k_x component of the Weyl points.

For the case of straight Fermi arcs ($d = 0$) with $\theta = 0$, the conductance reduces to $G_0 = 2Le^2\rho_0v_0$. As the Fermi arcs are tilted by a finite angle $\theta \neq 0$, we have $v_x^I = v_x^{\text{II}}$ and $v_z^I = -v_z^{\text{II}}$, which results in perfect negative refraction [cf. Fig. 1(d)]. As a result, the conductance is completely switched off by the gradient gate voltage, thus realizing a WEYL FET. This result also holds true when finite dispersion is added in the form of $\varepsilon_I = -\varepsilon_{\text{II}}$. In this case, due to the existence of reflection, the negative refraction is imperfect for small θ , and results in a finite switch-off angle θ_0 , see Fig 2(a)[38].

We also investigate the case with equal dispersion, i.e., $\varepsilon_I = \varepsilon_{\text{II}}$. In this case, the conductance G becomes a function of the tilting angle θ , see Fig. 2(b)[39]. G decreases with θ , indicating the suppression of transport by negative refraction. Whereas for straight Fermi arcs, G exhibits a sharp switch-off, as the dispersion strength increases, the current carried by refracted electrons cannot cancel out the incident current, resulting in a net current, which reduces the on/off ratio of the transistor for small θ .

Complementary to the 2D surface negative refraction analysis above, the on/off switch of the WEYL FET conductance can be understood by studying the 1D band structure of the nanowire. We map the Hamiltonian (1) onto a cubic lattice through the substitutions $k_i \rightarrow a^{-1} \sin k_i a$, $k_i^2 \rightarrow 2a^{-2}(1 - \cos k_i a)$, with a being the lattice constant. We can then solve the model and plot its energy bands using KWANT [40]. In Fig. 3, we compare the resulting band structures with and without the tilt of the Fermi arcs. For $\theta = 0$, the energy bands contributed by the surface states are gapless, indicating a metallic phase. For finite tilting angle θ , a gap opening occurs for the surface states, and the conduction is switched off for small bias voltages. Therefore, under a small bias voltage, the WEYL FET corresponds to a gate-tunable gap closing and opening in the 1D picture, which is consistent with the 2D picture of negative refraction, cf. Fig. 1(d).

Next, we numerically calculate the conductance through the nanowire based on the cubic lattice model [40]. We introduce surface dispersion using an

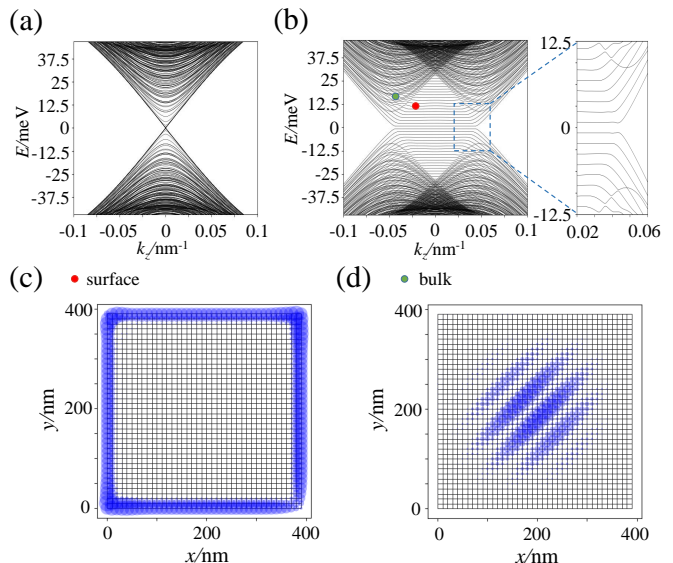


FIG. 3. Band structure of the Weyl nanowire for (a) $\theta = 0$ and (b) $\theta = \pi/6$, numerically calculated with a cross section of 40×40 sites. Spatial distribution of (c) a surface state and (d) a bulk state. Parameters used are $a = 10\text{nm}$, $k_0 = 0.1\text{nm}^{-1}$, $M = 4.375\text{eV}\cdot\text{nm}^2$ and $v = 10^6\text{m/s}$.

on-site potential U on the surface layer; because the surface states have a \mathbf{k} -dependent spatial distribution perpendicular to the surface, the on-site potential leads to a \mathbf{k} -dependent potential, or equivalently to an effective dispersion of the Fermi arcs. The conductance along the nanowire as a function of the tilting angle θ of the Fermi arcs is shown in Figs. 4(a) and (b). In Fig. 4(a), the onsite potential U takes opposite values on adjacent surfaces. Therefore, the dispersion on adjacent surfaces also takes opposite values, i.e., $\varepsilon_I = -\varepsilon_{\text{II}}$, and the on/off effect is confirmed. The angle at which the conductance is completely switched off increases with the onsite potential U , because curved Fermi arcs imply that reflection processes exist in addition to negative refraction for small θ . Hence, in order to realize perfect negative refraction, the tilting angle must exceed a critical value, cf. Fig. 2(a). In Fig. 4(b), the onsite potential U takes the same value on all surfaces, and the dispersions on the surfaces also become the same, i.e., $\varepsilon_I = \varepsilon_{\text{II}}$. As a result, the on/off ratio is reduced as U increases, which is in good agreement with the results in Fig. 2(b). Note that, here too, the surface dispersion has an adverse effect on the WEYL FET performance, which reduces the on/off ratio of the device. Therefore, in order to make a WEYL FET with high efficiency, it is preferable to use Weyl semimetals with weak and opposite surface dispersion. Recent experiments have realized Fermi arc manipulation by surface decoration [41, 42], which paves the way to realize our proposal.

In real materials, surface roughness is unavoidable, and we simulate this effect by including surface disorder. For

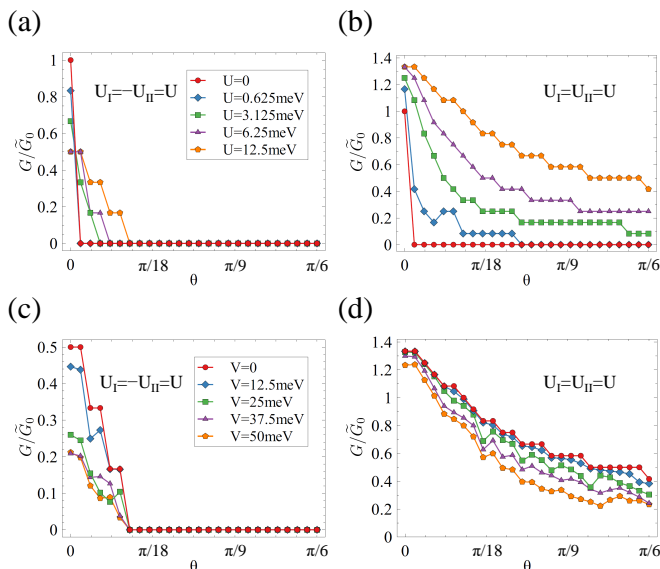


FIG. 4. Numerical simulation of adverse effect to the WEYL FET performance. (a) and (b): The conductance G for different surface dispersions renormalized by \tilde{G}_0 with $U = 0, \theta = 0$. (c) and (d): The conductance G in the presence of surface disorder with $U = 12.5$ meV. All other parameters are the same as those in Fig. 3.

\mathcal{P} -symmetric Weyl semimetals, the corresponding chiral surface states imply that electronic transport is immune to surface disorder, i.e., the functionality of the WEYL FET should be robust to disorder. In Figs. 4(c) and (d), we present the calculated device conductance under different surface disorder strength V for both dispersion configurations ($U_I = \pm U_{II}$). In both cases, the conductance decreases as surface disorder becomes stronger. This stems from the enhancement of backscattering that is induced by the disorder. However, the surface disorder has no effect on the switch-off region in Fig. 4(c), where perfect negative refraction occurs. In other words, the surface disorder has little effect on the functionality of the WEYL FET and the on/off ratio remains almost the same.

So far, we have solely analyzed a minimal \mathcal{P} -symmetric Weyl semimetal containing two Weyl points. Onto this minimal model, we have introduced the general principle of gate tunable Fermi arc tilting that can lead to negative refraction. Nevertheless, further work will analyze even more realistic situations, including (i) Weyl semimetals with multiple pairs of Weyl points, as in most of the materials [21–32]; here the geometry of the nanowire should be properly chosen such that the overlap between the projections of different Fermi arcs to the z -axis is minimized. Otherwise, the reflection at the boundary between different surfaces reduces the potency of negative refraction, and accordingly the on/off ratio of the WEYL FET. (ii) For time-reversal symmetric Weyl semimetals, the Fermi arc states are not chiral, leading to enhanced backscat-

tering. In this case, we expect that surface disorder will have a stronger impact, and will reduce the on/off ratio of the WEYL FET. Hence, for the time-reversal symmetric Weyl semimetal, a nanowire with a clean surface is required for a high-efficiency WEYL FET. (iii) Another adverse effect can arise from the deviation of the Fermi level from the bulk Weyl points. In this case, bulk electrons participate in the transport and contribute an overall background to the conductance, which reduces the on/off ratio of the WEYL FET. At the same time, multiple scattering may occur in the bulk states, which also increases the dissipation of the WEYL FET. Furthermore, the finite bulk density of states also brings considerable screening effect, which reduces the efficiency of the slanted gate voltage. Based on these observations, ideal Weyl semimetals are needed for efficient WEYL FETs [35, 36], similar to their vital role in measuring other properties of Weyl semimetals. (iv) Finally, in many Weyl semimetals, the Fermi arcs' dispersion is complex, making these surface states not much different from 2D normal metals, which cannot be used for WEYL FETs. Consequently, the material candidate for the WEYL FET should contain short Fermi arcs with small curvature [43–45].

In summary, we have explored a possible application of Weyl semimetal as a field-effect transistor (WEYL FET) that is based on electronic negative refraction between Fermi arcs on the surface of the device. By using the gradient gate along the Weyl nanowire, an on/off switch of the conductance can be achieved with a high ratio. Ideal Weyl semimetals with vanishing bulk density of states, chiral surface channels and small Fermi arc curvature can serve as good candidates for such high-efficiency WEYL FET with low-power consumption.

We acknowledge financial support from the Swiss National Science Foundation (SNSF) through Division II and the Careers Division.

* pchenweis@gmail.com

- [1] Carlos Galup-Montoro *et al.*, *MOSFET modeling for circuit analysis and design* (World scientific, 2007).
- [2] Ali Javey, Jing Guo, Qian Wang, Mark Lundstrom, and Hongjie Dai, “Ballistic carbon nanotube field-effect transistors,” *nature* **424**, 654 (2003).
- [3] Frank Schwierz, “Graphene transistors,” *Nature nanotechnology* **5**, 487 (2010).
- [4] F. D. M. Haldane, “Model for a quantum hall effect without landau levels: Condensed-matter realization of the “parity anomaly”,” *Phys. Rev. Lett.* **61**, 2015–2018 (1988).
- [5] Chao-Xing Liu, Xiao-Liang Qi, Xi Dai, Zhong Fang, and Shou-Cheng Zhang, “Quantum anomalous hall effect in $\text{Hg}_{1-y}\text{Mn}_y\text{Te}$ quantum wells,” *Phys. Rev. Lett.* **101**, 146802 (2008).
- [6] R. Yu, W. Zhang, H.-J. Zhang, S.-C. Zhang, X. Dai, and Z. Fang, “Quantized anomalous hall effect in magnetic

- topological insulators,” *Science* **329**, 61–64 (2010).
- [7] M Zahid Hasan and Charles L Kane, “Colloquium: topological insulators,” *Reviews of modern physics* **82**, 3045 (2010).
- [8] Xiao-Liang Qi and Shou-Cheng Zhang, “Topological insulators and superconductors,” *Reviews of Modern Physics* **83**, 1057 (2011).
- [9] C.-Z. Chang, J. Zhang, X. Feng, J. Shen, Z. Zhang, M. Guo, K. Li, Y. Ou, P. Wei, L.-L. Wang, Z.-Q. Ji, Y. Feng, S. Ji, X. Chen, J. Jia, X. Dai, Z. Fang, S.-C. Zhang, K. He, Y. Wang, L. Lu, X.-C. Ma, and Q.-K. Xue, “Experimental observation of the quantum anomalous hall effect in a magnetic topological insulator,” *Science* **340**, 167–170 (2013).
- [10] Chao-Xing Liu, Shou-Cheng Zhang, and Xiao-Liang Qi, “The quantum anomalous hall effect: Theory and experiment,” *Annual Review of Condensed Matter Physics* **7**, 301–321 (2016).
- [11] Xi-Rong Chen, Wei Chen, L. B. Shao, and D. Y. Xing, “Engineering chiral edge states in two-dimensional topological insulator/ferromagnetic insulator heterostructures,” *Phys. Rev. B* **99**, 085417 (2019).
- [12] Xiangang Wan, Ari M Turner, Ashvin Vishwanath, and Sergey Y Savrasov, “Topological semimetal and fermi-arc surface states in the electronic structure of pyrochlore iridates,” *Physical Review B* **83**, 205101 (2011).
- [13] Shuichi Murakami, “Phase transition between the quantum spin hall and insulator phases in 3d: emergence of a topological gapless phase,” *New Journal of Physics* **9**, 356 (2007).
- [14] A. A. Burkov and Leon Balents, “Weyl semimetal in a topological insulator multilayer,” *Phys. Rev. Lett.* **107**, 127205 (2011).
- [15] Zhijun Wang, Hongming Weng, Quansheng Wu, Xi Dai, and Zhong Fang, “Three-dimensional dirac semimetal and quantum transport in cd 3 as 2,” *Physical Review B* **88**, 125427 (2013).
- [16] Hongming Weng, Chen Fang, Zhong Fang, B. Andrei Bernevig, and Xi Dai, “Weyl semimetal phase in noncentrosymmetric transition-metal monophosphides,” *Phys. Rev. X* **5**, 011029 (2015).
- [17] Shin-Ming Huang, Su-Yang Xu, Ilya Belopolski, Chi-Cheng Lee, Guoqing Chang, BaoKai Wang, Nasser Alidoust, Guang Bian, Madhab Neupane, Chenglong Zhang, *et al.*, “A weyl fermion semimetal with surface fermi arcs in the transition metal monopnictide taas class,” *Nature communications* **6**, 7373 (2015).
- [18] Kai-Yu Yang, Yuan-Ming Lu, and Ying Ran, “Quantum hall effects in a weyl semimetal: Possible application in pyrochlore iridates,” *Phys. Rev. B* **84**, 075129 (2011).
- [19] Ching-Kit Chan, Netanel H. Lindner, Gil Refael, and Patrick A. Lee, “Photocurrents in weyl semimetals,” *Phys. Rev. B* **95**, 041104 (2017).
- [20] Gavin B Osterhoudt, Laura K Diebel, Mason J Gray, Xu Yang, John Stanco, Xiangwei Huang, Bing Shen, Ni Ni, Philip JW Moll, Ying Ran, *et al.*, “Colossal mid-infrared bulk photovoltaic effect in a type-i weyl semimetal,” *Nature materials* **18**, 471 (2019).
- [21] BQ Lv, HM Weng, BB Fu, XP Wang, Hu Miao, Junzhang Ma, P Richard, XC Huang, LX Zhao, GF Chen, *et al.*, “Experimental discovery of weyl semimetal taas,” *Physical Review X* **5**, 031013 (2015).
- [22] Su-Yang Xu, Ilya Belopolski, Nasser Alidoust, Madhab Neupane, Guang Bian, Chenglong Zhang, Raman Sankar, Guoqing Chang, Zhujun Yuan, Chi-Cheng Lee, *et al.*, “Discovery of a weyl fermion semimetal and topological fermi arcs,” *Science* **349**, 613–617 (2015).
- [23] Su-Yang Xu, Nasser Alidoust, Ilya Belopolski, Zhujun Yuan, Guang Bian, Tay-Rong Chang, Hao Zheng, Vladimir N Strocov, Daniel S Sanchez, Guoqing Chang, *et al.*, “Discovery of a weyl fermion state with fermi arcs in niobium arsenide,” *Nature Physics* **11**, 748 (2015).
- [24] Su-Yang Xu, Ilya Belopolski, Daniel S Sanchez, Chenglong Zhang, Guoqing Chang, Cheng Guo, Guang Bian, Zhujun Yuan, Hong Lu, Tay-Rong Chang, *et al.*, “Experimental discovery of a topological weyl semimetal state in tap,” *Science advances* **1**, e1501092 (2015).
- [25] Nan Xu, HM Weng, BQ Lv, Christian E Matt, Jihwey Park, Federico Bisti, Vladimir N Strocov, Dariusz Gawryluk, Ekaterina Pomjakushina, Kazimierz Conder, *et al.*, “Observation of weyl nodes and fermi arcs in tantalum phosphide,” *Nature communications* **7**, 11006 (2016).
- [26] Ke Deng, Guoliang Wan, Peng Deng, Kenan Zhang, Shijie Ding, Eryin Wang, Mingzhe Yan, Huaqing Huang, Hongyun Zhang, Zhilin Xu, *et al.*, “Experimental observation of topological fermi arcs in type-ii weyl semimetal mote 2,” *Nature Physics* **12**, 1105 (2016).
- [27] LX Yang, ZK Liu, Yan Sun, Han Peng, HF Yang, Teng Zhang, Bo Zhou, Yi Zhang, YF Guo, Marein Rahn, *et al.*, “Weyl semimetal phase in the non-centrosymmetric compound taas,” *Nature physics* **11**, 728 (2015).
- [28] Lunan Huang, Timothy M McCormick, Masayuki Ochi, Zhiying Zhao, Michi-To Suzuki, Ryotaro Arita, Yun Wu, Daixiang Mou, Huibo Cao, Jiaqiang Yan, *et al.*, “Spectroscopic evidence for a type ii weyl semimetallic state in mote 2,” *Nature materials* **15**, 1155 (2016).
- [29] Anna Tamai, QS Wu, Irène Cucchi, Flavio Yair Bruno, Sara Riccò, TK Kim, M Hoesch, Céline Barreteau, Enrico Giannini, Céline Besnard, *et al.*, “Fermi arcs and their topological character in the candidate type-ii weyl semimetal mote 2,” *Physical Review X* **6**, 031021 (2016).
- [30] Juan Jiang, ZK Liu, Y Sun, HF Yang, CR Rajamathi, YP Qi, LX Yang, C Chen, H Peng, CC Hwang, *et al.*, “Signature of type-ii weyl semimetal phase in mote 2,” *Nature communications* **8**, 13973 (2017).
- [31] Ilya Belopolski, Daniel S Sanchez, Yukiaki Ishida, Xingchen Pan, Peng Yu, Su-Yang Xu, Guoqing Chang, Tay-Rong Chang, Hao Zheng, Nasser Alidoust, *et al.*, “Discovery of a new type of topological weyl fermion semimetal state in mo x w 1- x te 2,” *Nature communications* **7**, 13643 (2016).
- [32] BQ Lv, N Xu, HM Weng, JZ Ma, P Richard, XC Huang, LX Zhao, GF Chen, CE Matt, F Bisti, *et al.*, “Observation of weyl nodes in taas,” *Nature Physics* **11**, 724 (2015).
- [33] Guangze Chen, Wei Chen, and Oded Zilberberg, “Negative refraction in fermi arc surface states of weyl semimetals,” in preparation (2019).
- [34] Hailong He, Chunyin Qiu, Liping Ye, Xiangxi Cai, Xiying Fan, Manzhu Ke, Fan Zhang, and Zhengyou Liu, “Topological negative refraction of surface acoustic waves in a weyl phononic crystal,” *Nature* **560**, 61 (2018).
- [35] Jiawei Ruan, Shao-Kai Jian, Hong Yao, Haijun Zhang, Shou-Cheng Zhang, and Dingyu Xing, “Symmetry-protected ideal weyl semimetal in hgte-class materials,” *Nature communications* **7**, 11136 (2016).
- [36] Jiawei Ruan, Shao-Kai Jian, Dongqin Zhang, Hong

- Yao, Haijun Zhang, Shou-Cheng Zhang, and Dingyu Xing, “Ideal weyl semimetals in the chalcopyrites cutlse_2 , agtlte_2 , autlte_2 , and znpbas_2 ,” *Phys. Rev. Lett.* **116**, 226801 (2016).
- [37] Wei Chen, Liang Jiang, R Shen, L Sheng, BG Wang, and DY Xing, “Specular andreev reflection in inversion-symmetric weyl semimetals,” *EPL (Europhysics Letters)* **103**, 27006 (2013).
- [38] The switch-off angle θ_0 is given by $\theta_0 = \arctan \frac{v_0}{\sqrt{2}k_0d}$ for the effective Hamiltonian Eq.(2).
- [39] For curved Fermi arcs and small θ , there exist reflection processes in addition to the negative refraction. Here, the reflection does not change v_z , and we calculate \bar{v}_z by $\bar{v}_z = \int_{-k_x^0}^{k_x^1} \frac{dk_x}{2k_x^0} \frac{v_z^I v_x^I + v_z^II v_x^I}{v_x^I + v_x^II} + \int_{k_x^1}^{k_x^0} \frac{dk_x}{2k_x^0} v_z^I$, where $k_x^1 = -k_0 \sin \theta / \sqrt{1 + \sin^2 \theta} + \hbar v_0 \cos \theta / d$ separates the Fermi arc into two segments which lead to negative refraction and reflection, respectively.
- [40] Christoph W Groth, Michael Wimmer, Anton R Akhmerov, and Xavier Waintal, “Kwant: a software package for quantum transport,” *New Journal of Physics* **16**, 063065 (2014).
- [41] HF Yang, LX Yang, ZK Liu, Y Sun, C Chen, H Peng, M Schmidt, D Prabhakaran, BA Bernevig, C Felser, *et al.*, “Topological lifshitz transitions and fermi arc manipulation in weyl semimetal nbas,” *Nature communications* **10**, 1–7 (2019).
- [42] Noam Morali, Rajib Batabyal, Pranab Kumar Nag, Enke Liu, Qiunan Xu, Yan Sun, Binghai Yan, Claudia Felser, Nurit Avraham, and Haim Beidenkopf, “Fermi-arc diversity on surface terminations of the magnetic weyl semimetal co3sn2s2 ,” arXiv preprint arXiv:1903.00509 (2019).
- [43] Jiaheng Li, Yang Li, Shiqiao Du, Zun Wang, Bing-Lin Gu, Shou-Cheng Zhang, Ke He, Wenhui Duan, and Yong Xu, “Intrinsic magnetic topological insulators in van der waals layered mnbi2te4-family materials,” *Science Advances* **5**, eaaw5685 (2019).
- [44] Lin-Lin Wang, Na Hyun Jo, Brinda Kuthanazhi, Yun Wu, Robert J. McQueeney, Adam Kaminski, and Paul C. Canfield, “Single pair of weyl fermions in the half-metallic semimetal EuCd_2As_2 ,” *Phys. Rev. B* **99**, 245147 (2019).
- [45] J-R Soh, F de Juan, MG Vergniory, NBM Schröter, MC Rahn, DY Yan, M Bristow, PA Reiss, JN Blandy, YF Guo, *et al.*, “An ideal weyl semimetal induced by magnetic exchange,” arXiv preprint arXiv:1901.10022 (2019).